Int. J. Heat Mass Transfer. Vol. 12, pp. 1182–1187. Pergamon Press 1969. Printed in Great Britain

HEAT TRANSFER IN A TUBE WITH FORCED CONVECTION, INTERNAL RADIATION EXCHANGE, AXIAL WALL HEAT CONDUCTION AND ARBITRARY WALL HEAT GENERATION

R. S. THORSEN

Assistant Professor, Dept. of Mechanical Engineering, New York University, New York 10453

(*Received* 26 *August* 1968 *and in revised form* 26 *February* 1969)

NOMENCLATURE

A_w, tube cross-sectional area, $\pi/4(D^2 - d^2)$;
B, radiosity;
d, D, inside, outside tube diameter;
k, thermal conductivity;
L^+, tube length;
N, $\ddot{q}_{av}d/T_i k$;
P, $k_w[(D/d)^2 - 1]\,(\ddot{q}_{av}/\sigma)^{\frac{1}{2}}/(4\ddot{q}_{av}d)$;
Pe, Peclet number;
Pr, Prandtl number;
$\ddot{q}$, tube wall heat generation per unit inside area;
$\ddot{q}_{av}$, average $\ddot{q}$ defined as $(1/L)\int_0^L \ddot{q}\,\mathrm{d}x$;
q_c, convection heat transfer rate per unit inside area;
Q_c, $q_c/\ddot{q}_{av}$;
Q_0, $B/\ddot{q}_{av}$;
r^+, radial coordinate;
r, $2r^+/d$;
Re, Reynolds number;
T, temperature;
x^+, axial coordinate measured from tube inlet;
x, x^+/d.

Greek symbols

ε, emissivity of inside tube surface;
η, ξ, dummy variables of integration;
θ, T/T_i;
σ, Stefan–Boltzmann constant;
τ, $T_i(\sigma/\ddot{q}_{av})^{\frac{1}{2}}$.

Subscripts

e, refers to tube exit;
i, refers to tube inlet;
w, refers to tube wall.

INTRODUCTION

THOUGH a number of analyses of internal flows with combined convection and radiation heat transfer have been presented in the literature, attention has been directed to the simplest case of the uniform temperature boundary condition with a few notable exceptions [1–4]. Not only is the uniform temperature boundary condition frequently inconsistent with reality, it is also difficult to achieve in the laboratory. On the other hand, uniform wall heat generation, which is a special case of the problem presented, can be approached quite accurately, e.g., by the passage of electric current through the tube wall.

The analyses of [1–3] are limited in that they require the convection coefficient to be specified *a priori*. In [1] and [2] the convection coefficient is assumed constant and in [3] it is taken to vary axially in an *a priori* known manner that is in agreement with analytic and experimental results in the absence of radiation exchange between the non-isothermal tube wall elements. Chen [4] analyzed laminar tube flow without any *a priori* assumption regarding the convection coefficient. However, in his analysis radiation effects are introduced by assuming that heat transfer to the gas at the tube wall is proportional to $T_w^4(x)$. As shown in [1–3] this is not correct since it neglects irradiation at x arriving from other elements of the non-isothermal wall. The present analysis is an attempt to overcome these two deficiencies in prior analyses.

ANALYSIS

A radiatively non-participating gas enters the tube shown in Fig. 1. The gas is assumed to enter at a uniform temperature T_i and has a fully developed velocity profile. All fluid properties are taken to be constant and the ends of the tube are considered to be black surfaces. As previously shown in [1–3] an energy balance on a tube ring at x, having cross-sectional area A_w and length $\mathrm{d}x$ results in

$$p\tau\frac{\mathrm{d}^2\theta_w}{\mathrm{d}x^2} + f(x) + \tau^4[F(x) + \theta_e^4 F(L - x)] + \int_0^L Q_0(\xi)K(x,\xi)\,\mathrm{d}\xi = Q_0(x) + Q_c(x) \qquad (1)$$

when $f(x) = \ddot{q}(x)/\ddot{q}_{av}$ is introduced. The dimensionless radiosity can be eliminated in terms of

$$Q_0 = \left[\left(\frac{1-\varepsilon}{\varepsilon}\right)\left(Q_c - f - p\tau\frac{d^2\theta_w}{dx^2}\right) + \tau^4\theta_w^4\right]. \quad (2)$$

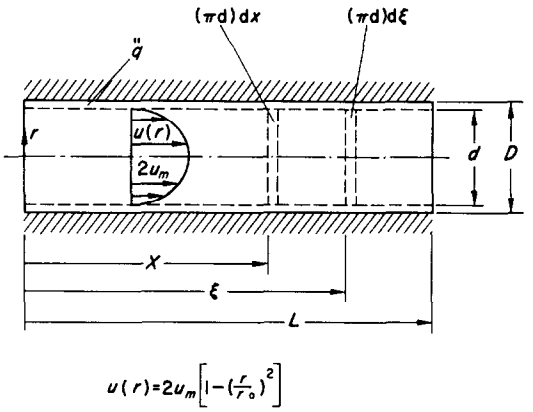

FIG. 1. Diagram of problem under consideration.

In equation (1) the first term accounts for axial wall conduction, the second for arbitrary wall heat generation and the third for radiation between an elementary ring at x and the tube ends. The integral arises from irradiation at x arriving from the remainder of the non-isothermal tube. Q_0 is the dimensionless net radiant energy leaving an element due to emission and reflection, i.e., the radiosity and Q_c is the dimensionless heat flux conducted to the gas at the tube wall-gas interface. The shape factor between a ring at x and a circular disk at the tube entrance, F, and the shape factor between a differential ring at x and ξ, K, are given respectively by

$$F(x) = (x^2 + \tfrac{1}{2})/(x^2 + 1)^{\frac{1}{2}} - x \quad (3)$$

and

$$K(x,\xi) = K(|x-\xi|) = 1 - |x-\xi|\,[(x-\xi)^2 + \tfrac{3}{2}]/[(x-\xi)^2 + 1]^{\frac{3}{2}}. \quad (4)$$

$\theta_w(x)$, $\theta_e(x)$, $Q_0(x)$ and $Q_c(x)$ are unknown in equations (1) and (2) and $f(x)$ can be arbitrarily prescribed. Additional equations are obtained by considering the gas. It is shown in [5] that

$$\theta(x,r) = 1 + \int_0^x \left\{1 - \Omega\left[\frac{2}{Pe}(x-\xi), r\right]\right\} d\theta_w \quad (5)$$

and

$$Q_c(x) = \frac{2}{N}\int_0^x G(x-\xi)\,d\theta_w. \quad (6)$$

For laminar flow, Ω appearing in the Stieljes integral of equation (5) is the solution to the classical Graetz problem and $G(x-\xi)$, has been introduced in place of $-\Omega_r[2/Pe\,(x-\xi), 1]$ for compactness in equation (6).

It is shown in [5] that

$$G(x-\xi) = 2{\cdot}02552\sum_{n=0}^{\infty}\lambda_n^{-\frac{1}{3}}\exp.\left[-\frac{2}{Pe}\lambda_n^2(x-\xi)\right] \quad (7)$$

and

$$\lambda_0 = 2{\cdot}704, \quad \lambda_1 = 6{\cdot}679, \quad \lambda_n = 4n + \tfrac{8}{3} \text{ for } n \geqslant 2.$$

Finally, the axial variation of the fluid bulk temperature, $\theta_b(x)$, is given by

$$\theta_b(x) = 1 + \frac{4N}{Pe}\int_0^x Q_c\,d\xi. \quad (8)$$

Setting $x = L$ in equation (8) determines θ_e.

Combining equations (1), (2) and (6) results in a single integro-differential equation, viz:

$$\frac{p\tau}{\varepsilon}\frac{d^2\theta_w}{dx^2} + \frac{f(x)}{\varepsilon} + \tau^4[F(x) + \theta_e^4 F(L-x)] + \int_0^L\left\{\left(\frac{1-\varepsilon}{\varepsilon}\right)\left[\frac{2}{N}\int_0^\xi G(\xi-\eta)\frac{d\theta_w}{d\eta}d\eta + \frac{2}{N}G(\xi-0)(\theta_w(0)-1) - f(\xi) - p\tau\frac{d^2\theta_w}{d\xi^2}\right] + \tau^4\theta_w^4\right\}K(x,\xi)\,d\xi = \frac{2}{\varepsilon N}\int_0^x G(x-\xi)\frac{d\theta_w}{d\xi}d\xi + \frac{2}{\varepsilon N}G(x-0).[\theta_w(0)-1] + \tau^4\theta_w^4. \quad (9)$$

In arriving at equation (9) due consideration has been given to the discontinuity between the wall and fluid temperature that will arise at $x = 0$ when the boundary conditions

$$\frac{d\theta_w}{dx} = 0, \quad x = 0, \quad x = L \quad (10)$$

are imposed. This is reflected in the terms containing $\theta_w(0) - 1$.

It is noted that one term in equation (9) is a double integral which will require special consideration before attempting a solution. Recalling that $K(x,\xi) = K(|x-\xi|)$ define

$$A(x) = \int_0^L\int_0^\xi K(|x-\xi|)\,G(\xi-\eta)\frac{d\theta_w}{d\eta}d\eta\,d\xi. \quad (11)$$

The domain of integration $\hat{D}$, defined by the limits of integration in equation (11) is shown in figure (2). Reversing the order of integration results in

$$A(x) = \int_0^x \phi_1(x,\eta)\frac{d\theta_w}{d\eta}d\eta + \int_x^L \phi_2(x,\eta)\frac{d\theta_w}{d\eta}d\eta \qquad (12)$$

where

$$\phi_1(x,\eta) = \int_\eta^x K(x-\xi)\,G(\xi-\eta)\,d\xi + \int_x^L K(\xi-x)\,G(\xi-\eta)\,d\xi \qquad (13)$$

$$\phi_2(x,\eta) = \int_\eta^L K(\xi-x)\,G(\xi-\eta)\,d\xi. \qquad (14)$$

Equations (12), (13) and (14) were arrived at by dividing the integration over $\hat{D}$ into integration over domains I, II and III in Fig. 2 and recognizing that

$$K(|x-\xi|) = \begin{cases} K(x-\xi), & x \geqslant \xi \\ K(\xi-x), & x < \xi. \end{cases} \qquad (15)$$

Substituting equation (12) into (9) and performing algebraic rearrangement yields

$$p\tau\frac{d^2\theta_w}{dx^2} + S(x) - \varepsilon\tau^4\theta_w^4 + \left\{[\theta_w(0)-1] \times \left[(1-\varepsilon)\frac{2}{N}\phi_1(x,0) - \frac{2}{N}G(x-0)\right]\right\} + \int_0^x \left[(1-\varepsilon)\left(\frac{2}{N}\right)\phi_1(x,\xi)\frac{d\theta_w}{d\xi} - (1-\varepsilon)(p\tau)K(x-\xi) \times \frac{d^2\theta_w}{d\xi^2} - \frac{2}{N}G(x-\xi)\frac{d\theta_w}{d\xi} + \varepsilon\tau^4 K(x-\xi)\theta_w^4\right]d\xi + \int_0^L \left[(1-\varepsilon)\left(\frac{2}{N}\right)\phi_2(x,\xi)\frac{d\theta_w}{d\xi} - (1-\varepsilon)(p\tau)K(\xi-x) \times \frac{d^2\theta_w}{d\xi^2} + \varepsilon\tau^4 K(\xi-x)\theta_w^4\right]d\xi = 0. \qquad (16)$$

$S(x)$ appearing in (16) is a known function of x given by

$$S(x) = f(x) - (1-\varepsilon)\int_0^L K(|x-\xi|)\,f(\xi)\,d\xi + \varepsilon\tau^4[F(x) + \theta_e^4\,F(L-x)]. \qquad (17)$$

Equation (16) is in many respects quite similar to equation (B3) of [3]. However, the present formulation has the virtue of allowing for an arbitrary wall heat generation and the convection coefficient is not assumed *a priori*.

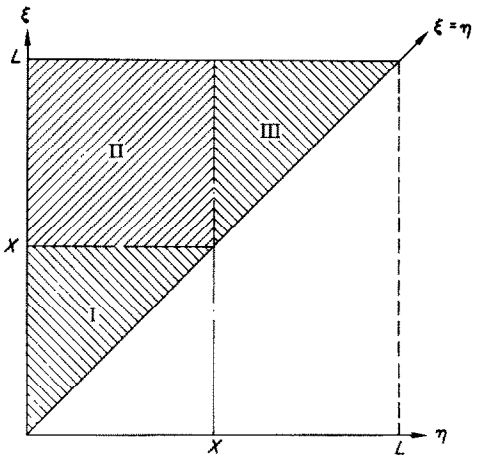

FIG. 2. Division of $\hat{D}$ into three domains of integration for evaluation of $A(x)$.

The task is now to evaluate $\theta_w(x)$ from equation (16). To this end $S(x)$, $\phi_1(x,\xi)$ and $\phi_2(x,\xi)$ must be evaluated explicitly. For purposes of illustration laminar flow with a fully-developed velocity profile and uniform wall heat generation will be assumed, i.e., $f(x)$ is taken to be 1. With $f(x) = 1$,

$$S(x) = \varepsilon + (1-\varepsilon+\varepsilon\tau^4)F(x) + (1-\varepsilon+\varepsilon\tau^4\theta_e^4) \times F(L-x). \qquad (18)$$

Determination of ϕ_1 and ϕ_2 requires evaluating expressions of the form

$$J_n(x,\eta) = \exp[-a_n(x-\eta)]\int_\eta^x K(s)\exp(a_n s)\,ds \qquad (19)$$

where $a_n = 2\lambda_n^2/Pe$. Numerical evaluation of these integrals can be avoided by noting that $K(s)$ has the same qualitative behavior as $\hat{K}(s) = \exp(-cs)$.

The criterion for selecting c such that $\hat{K}(s) \approx K(s)$ is somewhat arbitrary. However, it is to be noted that for $s > 2$ $\hat{K}(s)$ and $K(s)$ differ by less than 0·002 when $c > 2$. Furthermore, it is not $K(s)$ that must be approximated accurately; rather, it is the J_n's that must be accurately approximated when K is replaced by $\hat{K}$. The error introduced into the J_n's by approximating K by $\hat{K}$ will depend on a_n and the limits of integration. It will be greatest for small a_n and small limits of integration. The smallest value of a_n to be encountered is $a_0 = 2\lambda_0^2/1400 \approx 0{\cdot}01$. Thus, c is determined by requiring

$$\int_0^2 K(s)\,e^{0{\cdot}01s}\,ds = \int_0^2 e^{-cs}\,e^{0{\cdot}01s}\,ds. \qquad (20)$$

The integral on the left of equation (20) is evaluated numerically, resulting in a value of $c = 2$. The accuracy of this approximation is shown in Fig. 3.

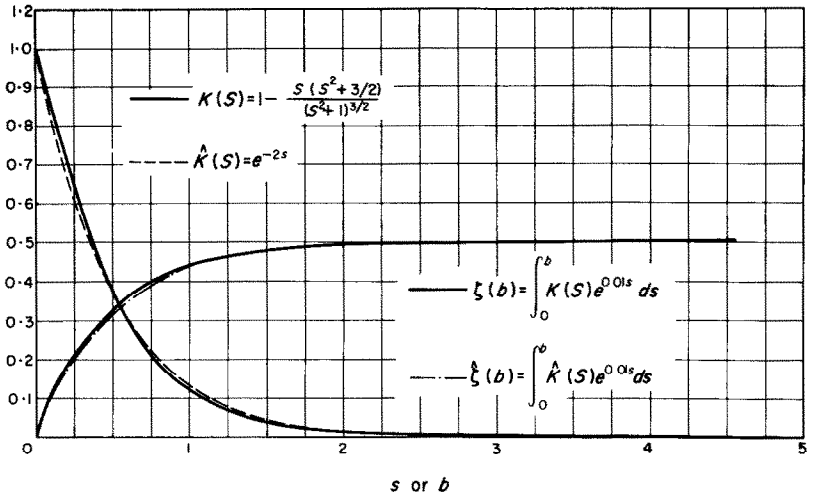

FIG. 3. Accuracy of approximating $K(s)$ by $\hat{K}(s)$.

SOLUTION OF GOVERNING EQUATION

The solution of equation (16) subject to the constraints imposed by (10) and the condition

$$\theta_e = 1 + \frac{4N}{Pe}\int_0^L Q_c\,d\xi \tag{21}$$

was achieved numerically on a C.D.C. 6600 digital computer. The tube was divided into 30 equal axial increments of length, δ, to allow computation of the wall temperature at 31 points. The linear integrals appearing in (16) were evaluated as sums of integrals over the appropriate number of divisions. For example, at the ith axial point

$$\int_0^{x_i}\phi_1(x_i,\xi)\frac{d\theta_w}{d\xi}d\xi = \sum_{j=1}^{i-1}\int_{x_j}^{x_{j+1}}\phi_1(x_i,\xi)\frac{d\theta_w}{d\xi}d\xi \tag{22}$$

where $x_1 = 0$. For each interval the mean value theorem for integrals was applied, resulting in

$$\int_0^{x_i}\phi_1(x_i,\xi)\frac{d\theta_w}{d\xi}d\xi = \sum_{j=1}^{i-1}\phi_1(x_i\bar{\xi}_j)[\theta_w(x_{j+1})-\theta_w(x_j)]. \tag{23}$$

From the mean value theorem $x_j < \bar{\xi}_j < x_{j+1}$, and $\bar{\xi}_j$ was arbitrarily taken as $(x_j + x_{j+1})/2$.

To accurately evaluate the non-linear integrals in (16) without introducing additional nodes, a composite quadrature formula was used. Specifically, each interval $x_j \leqslant \xi \leqslant x_{j+1}$ was divided into three sub-intervals and a closed Newton–Cotes formula with a Lagrange interpolation polynomial was used. In the resulting formula, the integrand, $K(|x_i - \xi|)\,\theta_w^4$, had to be known at two intermediate points in the jth interval, $x_j + (\delta/3)$ and $x_j + (2\delta/3)$. $K(|x_i - \xi|)$ was known exactly at these points and consistent with the difference approximations for the various derivatives arising in (16), a straight line approximation was used to relate $\theta_w[x_j + (\delta/3)]$ and $\theta_w[x_j + (2\delta/3)]$ to $\theta_w(x_j)$ and $\theta_w(x_j + 1)$. With these estimates for the integrals and a central difference approximation for the second derivative, equation (16) was reduced to a system of 31 algebraic equations,

$$\sum_{j=1}^{31} b_{ij}\,\theta_{wj} = -S(x_i) + \varepsilon\tau^4\,[\theta_{w_i}^4 - \sum_{j=1}^{30} X_{ij}(\theta_{w_j}, \theta_{w_{j+1}})]. \tag{24}$$

In (24) linear terms in the dependent variable appear on the left and $X_{ij}(\theta_{wj}, \theta_{wj+1})$ arose from the non-linear integrals and depends in a non-linear manner on its arguments.

Due to its non-linearity, equation (24) was solved iteratively. Initially, $\theta_w(x)$ was taken as the solution to (16) neglecting all radiation terms and a value assumed for θ_e. These trial values were used to evaluate the right hand side of (24) and the Gauss elimination method used to determine new values of $\theta_w(x_i)$, and θ_e was checked by integrating (6) and (21). The iteration procedure terminated when no dimensionless temperature changed by more than 0·01.

RESULTS AND CONCLUSIONS

Because an analytic solution to equation (16) is not possible, the dependence of the solution, θ_w, on the parameters entering this equation cannot be studied completely. Therefore careful selection of the parameters is necessary prior to attempting a numerical solution. These parameters are P, τ, L/d, ε, N, Pe and the particular gas under considera-

tion. Air at 500°F was assumed to enter a $\frac{1}{4}$ in. i.d., $\frac{5}{16}$ in. o.d. tube and $\bar{q}$ was selected to assure large, but reasonable, wall temperatures. The tube thermal conductivity was selected to be representative of inconel and stainless steel at the low extreme and copper at the high extreme. In this manner P, τ and N were determined.

In the absence of radiation the convenient dimensionless length to use is $2x/Pe$. However, when radiation effects are present x enters explicitly. Therefore, values of L and Pe had to be specified separately. L was selected as 20 and 50 while Pe was taken as 280 and 1400 (corresponding to Reynolds numbers of 400 and 2000). Finally ε was taken as 1·0, 0·5 and 0·1. Because $\bar{q}$ enters τ only to the $-\frac{1}{4}$ power τ could not be varied significantly while retaining reasonable wall temperatures. Also, since for fixed flow conditions N changed in direct proportion to $\bar{q}$ it was essentially determined by the wall temperature range. Thus, only the effect of P, L/d, ε and Pe were studied carefully.

As expected, the effect of increasing the conduction parameter, P, was to reduce axial temperature gradients and the maximum temperature in the tube wall. The effect of emissivity and L is shown in Fig. 4.

A most interesting result is to be observed in the Nusselt number behavior shown in Fig. 4. For reference the uniform wall heat flux and uniform temperature Nusselt numbers for the Graetz problem [6] are presented. As expected, the results of the present analysis lie between these two curves near the tube entrance. However, as the tube exit is approached the present results continue to decrease (as opposed to approaching an asymptotic value) and eventually even become negative. This result could have been anticipated by examining equation (6). $G(x-\xi)$ is positive and largest when ξ is close to x. Thus, when $d\theta_w = (d\theta_w/d\xi)\,d\xi$ becomes negative the entire integral can become negative. Since θ_w remained greater than θ_b for the entire tube length, defining the convection coefficient as $q_c/(T_w - T_b)$ results in negative values of Nu. This unusual Nusselt number behavior was less pronounced for small values of ε and large values of P since the wall temperature variation was less severe under these conditions.

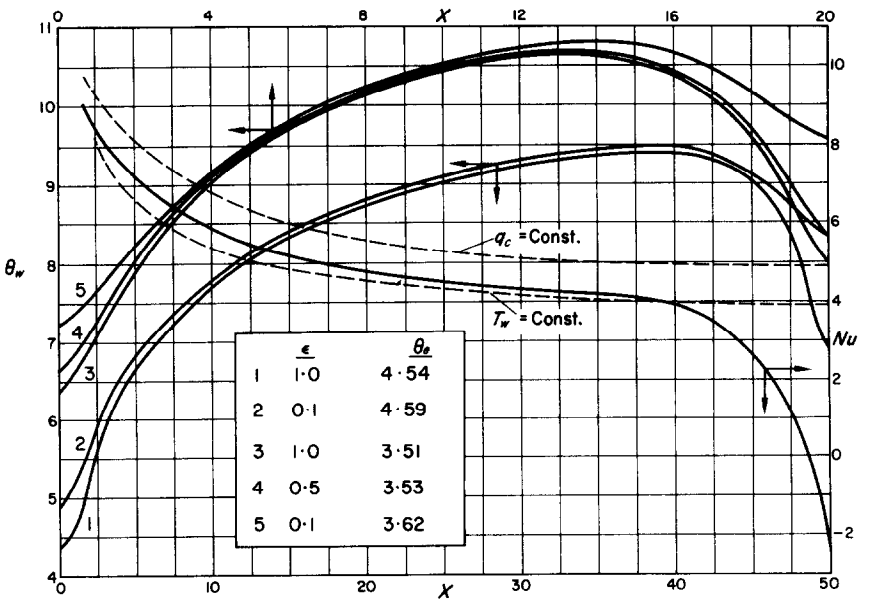

FIG. 4. Tube wall temperature distribution and Nusselt number variation, $Pe = 1400$.
Curves 1, 2: $L = 50$, $P = 6{\cdot}0$, $N = 28$, $\tau = 0{\cdot}27$.
Curves 1, 2, 3: $L = 20$, $P = 3{\cdot}0$, $N = 70$, $\tau = 0{\cdot}21$.

It is to be noted that a lower value of ε results in higher wall temperatures at the tube entrance and exit and smaller axial temperature gradients in the wall. This can be understood by recognizing that approximately the same energy is radiated out the tube ends for the three curves corresponding to $L = 20$ and the two curves for $L = 50$.

ACKNOWLEDGEMENTS

This research was performed under partial support from the National Science Foundation Institutional Grant to New York University. The author also wishes to acknowledge the cooperation of the Courant Institute of Mathematical Sciences at New York University for providing computer time for this work.

REFERENCES

1. M. PERLMUTTER and R. SIEGEL, Heat transfer by combined forced convection and thermal radiation in a heated tube, *Trans. Am. Soc. Mech. Engrs* (C), *J. Heat Transfer* **84**, 301–311 (1962).
2. R. SIEGEL and M. PERLMUTTER, Convective and radiant heat transfer for flow of a transparent gas in a tube with a gray wall. *Int. J. Heat Mass Transfer* **5**, 639–660 (1962).
3. R. SIEGEL and E. G. KESHOCK, Wall temperatures in a tube with forced convection, internal radiation exchange and axial wall heat conduction, NASA TN D-2116, March 1964.
4. J. C. CHEN, Laminar heat transfer in tube with nonlinear radiant heat-flux boundary condition, *Int. J. Heat Mass Transfer* **9**, 433–439.
5. J. SELLARS, M. TRIBUS, and J. KLEIN, Heat transfer to laminar flow in a round tube or flat conduit—the Graetz problem extended, *Trans. Am. Soc. Mech. Engrs* **78**, 441–448 (1956).
6. W. M. KAYS, *Convective Heat and Mass Transfer*, pp. 133–142. McGraw-Hill, New York (1966).

Int. J. Heat Mass Transfer. Vol. 12, pp. 1187–1191. Pergamon Press 1969. Printed in Great Britain

TEMPERATURE DISTRIBUTIONS FOR INSCRIBABLE NONCIRCULAR DUCTS HAVING CONSTANT WALL HEAT FLUX AND CONSTANT VELOCITY FLOW

JOSEPH T. PEARSON

School of Mechanical Engineering, Purdue University, Lafayette, Indiana, U.S.A.

(*Received* 26 *February* 1968 *and in revised form* 3 *February* 1969)

NOMENCLATURE

A,	cross-sectional area of duct;
A_i,	area subtended by the ith flat side of duct;
A_j,	area subtended by the jth curved side of duct;
B,	a constant;
e_i,	distance measured along the ith side of duct from a corner to the tangent point of the inscribed circle;
k,	thermal conductivity of fluid;
L_i,	width of the ith flat side of duct;
m,	total number of flat sides of an inscribable duct;
n,	total number of curved sides of an inscribable duct;
n,	inward normal to duct's surface;
P,	perimeter of duct's cross-section;
q_w,	wall heat flux at duct's inside surface;
r, θ, z,	cylindrical coordinates;
r_h,	hydraulic radius and radius of circle inscribed in duct's cross section, $r_h = 2A/P$;
$\overline{r^2}$,	square of radius of gyration of duct's cross-section;
$S(r, \theta) = 0$,	equation for duct's inside surface;
T,	temperature;
T_0,	temperature at duct's entrance;
t,	time;
u,	velocity of fluid in z direction;
v_r,	velocity of fluid in r direction;
v_θ,	velocity of fluid in θ direction;
x, y, z,	Cartesian coordinates;
Z,	thermal entrance length;
α,	thermal diffusivity of fluid.

Subscripts

b,	bulk temperature;
c,	center or axis of duct;
i,	the ith flat side;
j,	the jth curved side;
n,	normal to duct's surface;
0,	duct's entrance;
s,	at duct's surface;
1,	some point in fluid after thermal entrance region.

INTRODUCTION

FLUID flow passages in modern heat exchange systems are often of noncircular cross-sectional shape. In fact, heat transfer passages which are employed in aircraft, missiles, space vehicles and nuclear reactors are more often than not noncircular. In these engineering applications it is of utmost importance that the heat exchange systems operate as efficiently and as safely as possible. However, at the present time comprehensive design criteria which can be utilized to analyze the fluid mechanics and heat transfer associated with the various components of these systems are sparse. This is because it is quite difficult to simultaneously analyze the problem of combined fluid mechanics and heat transfer in irregularly shaped channels as has been pointed out by Sparrow and Haji-Sheikh [1] and Wilson and Medwell [2].

To ease this situation one often seeks to separate the heat